PHYSICAL REVIEW B VOLUME 15, NUMBER 7 1 APRIL 1977

Propagation of surface magnetoelastic waves on ferromagnetic crystal substrates*

R. Q. Scott and D. L. Mills
Department of Physics, University of California, Irvine, California 92717
(Received 3 May 1976)

We present a theoretical study of the propagation of surface acoustic waves on a ferromagnetic crystal in the presence of magnetoelastic coupling. For parameters characteristic of YIG, with the sample magnetization and Zeeman field parallel to the surface, we examine the dispersion and attenuation of waves propagating in an arbitrary direction relative to the magnetization. In addition we detail the behavior of the polarization of the lattice motion and the demagnetizing fields set up by the wave. We study two distinct kinds of magnetoelastic surface waves: one is in essence a Rayleigh wave modified by the magnetoelastic coupling and the second a shearlike magnetoelastic surface wave that exists only in the presence of magnetoelastic coupling. These waves provide a short-wavelength probe of the Damon-Eshbach surface spin waves and of the nature of the bulk spin-wave eigenmodes near the surface.

I. INTRODUCTION

Rayleigh waves are the surface bound excitations of the elastic strain field of a solid and, in the presence of any small coupling, provide the opportunity of probing by acoustical means the nature of elementary excitations near the crystal surface. Consequently it is of interest of inquire into the coupling of surface acoustic waves on solids with other elementary excitations accessible to the Rayleigh-wave frequency range. This is of interest for two reasons. First of all, the wavelength of Rayleigh waves can readily be made small compared to the sample dimensions, and this is true also of the penetration depth, into the crystal, of its strain field. Thus, the Rayleigh wave can probe the nature of elementary excitations near the surface of a crystal under circumstances in which the medium may be regarded as semi-infinite. Also, if the Rayleigh wave couples to other low-frequency excitations, its properties may then be altered or manipulated (i.e., the attenuation rate or the dispersion of the wave may be altered through variation of external parameters).

We have examined the theory of surface acoustic-wave propagation on ferromagnetic substrates in the presence of coupling between the elastic strain field and the ferromagnetically aligned spins. It is via this magnetoelastic coupling that elastic disturbances in the solid excite the spin system giving rise, when supplemented by the appropriate boundary conditions, to the magnetoelastic surface modes to be discussed here.

We assume a geometry in which the magnetization and an externally applied dc magnetic field are parallel to the sample surface and the wave propagates in an arbitrary direction relative to the magnetization. We consider here a stress-free surface, unloaded by a conducting film.[1]

The propagation characteristics we find are highly geometry dependent, the angle between the sample magnetization and the wave vector being the critical parameter. We find that magnetoelastic waves of two sorts can be propagated. The waves of the first kind may be characterized as Rayleigh-like in terms of their lattice displacement patterns (they reduce to the Rayleigh wave in the limit of vanishing magnetoelastic coupling). The second solution, a quasishear mode, has no correspondence in elasticity theory and depends on the presence of magnetoelastic coupling for its existence. A striking feature of our results is the presence of nonreciprocity in the propagation characteristics, i.e., for a given frequency, the wave vector and attenuation length for propagation from right to left relative to the magnetic field differs from that for propagation from left to right. This we show to be a general feature of surface wave propagation with a magnetic field parallel to the surface.

We have calculated numerically the dispersion and attenuation lengths of these modes as well as the elastic displacement fields and magnetic field components associated with them. These calculations were done for material parameters characteristic of YIG.

Two particularly striking features are the strong interaction between the Rayleigh wave and the bulk spin waves as well as its coupling to the Damon-Eshbach surface spin waves. These are surface spin waves on a semi-infinite ferromagnet that exists at long wavelengths where dipolar coupling dominates the exchange interaction.[2] Thus the study of magnetoelastic surface wave propagation offers the unique possibility of studying the bulk spin-wave mode structure and the Damon-Eshbach surface spin waves with a probe of short wavelength, in contrast to microwave resonance studies

which probe only geometrical resonances of the entire sample. This may prove a useful method for studying the nature of the spin-pinning interactions near the surface of a ferromagnet. In principle, while we do not consider the effect of spin pinning here, both the coupling to the Damon-Eshbach wave as well as the interaction with the bulk spin-wave modes should be sensitive to its presence. Thus, we have here an example of the potential utility of Rayleigh waves as a short-wavelength probe of elementary excitations near crystal surfaces.

II. GENERAL THEORETICAL CONSIDERATIONS

We assume a semi-infinite ferromagnetic crystal which is taken to be elastically isotropic. The system of coordinates is oriented so that the crystal occupies the half-space $y>0$ with the magnetization $\vec{M}$ and an externally applied dc magnetic field $\vec{H}_0$ lying in the $\hat{z}$ direction. Note that the z axis is parallel to the surface. The wave then propagates with frequency Ω and wave vector $\vec{Q}$ ($\vec{Q}$ is parallel to the surface) at an angle θ relative to the magnetization vector (Fig. 1).

In the absence of magnetoelastic coupling the spin system obeys a Bloch equation:

$$\frac{d\vec{M}}{dt}=\gamma(\vec{M}\times\vec{H})-\frac{1}{\tau}\vec{M}\,. \tag{2.1}$$

Here γ is the gyromagnetic ratio and

$$\vec{H}=H_0\hat{z}+\vec{h}_d\,, \tag{2.2}$$

$\vec{h}_d$ being the demagnetizing field associated with the spin motion. The quantity τ is the transverse relaxation time of the spins.

The demagnetizing field $\vec{h}_d$ is to be calculated from the Maxwell equations. In typical surface acoustic-wave systems we are restricted to frequencies of a few GHz or less corresponding to wave vectors on the order of 10^5 cm^{-1}. Then we have $cQ \gg \Omega$, where c is the speed of light. Thus retardation effects can be ignored and we may use the magnetostatic approximation. Then Maxwell's equations become

$$\vec{\nabla}\cdot\vec{B}=\vec{\nabla}\times\vec{H}=0\,. \tag{2.3}$$

In the absence of magnetoelastic coupling the kth Cartesian component of elastic displacement u_k obeys

$$\rho\frac{\partial^2 u_k}{\partial t^2}=\sum_i\frac{\partial}{\partial x_i}\left(\frac{\partial\mathcal{H}}{\partial e_{ki}}\right), \tag{2.4}$$

where the e_{ki} are the elements of the strain tensor and $\mathcal{H}$ the Hamiltonian density appropriate to an isotropic elastic continuum, with mass density ρ and transverse and longitudinal sound velocities c_t and c_l, respectively.

The equations of motion (2.1) and (2.4) are now to be modified by including terms representing the contribution of the magnetoelastic coupling. For a ferromagnetic material of cubic symmetry, in the spin-wave regime where only the terms linear in the transverse magnetization are retained, the interaction Hamiltonian density is given by[3]

$$\mathcal{H}_{ls}=(b_2/M_s)[M_x(e_{xz}+e_{zx})+M_y(e_{yz}+e_{zy})]\,. \tag{2.5}$$

Here b_2 is a phenomenological coupling constant and M_s the saturation magnetization. M_x and M_y are the transverse components of the magnetization. The contributions to the spin equation of motion Eq. (2.1) can be calculated by noting the magnetoelastic coupling is equivalent to an additional effective magnetic field which drives the spin system. This effective field is $\vec{h}_{ls}$, where

$$\gamma\vec{h}_{ls}=-\hat{x}(b_2/M_s)(e_{xz}+e_{zx})-\hat{y}(b_2/M_s)(e_{yz}+e_{zy})\,. \tag{2.6}$$

The contributions of the magnetoelastic coupling to the lattice equation (2.4) are found by adding to the right-hand side the piece

$$\rho\left(\frac{\partial^2 u_k}{\partial t^2}\right)_{\rm me}=\sum_i\frac{\partial}{\partial x_i}\left(\frac{\partial\mathcal{H}_{ls}}{\partial e_{ki}}\right)\,. \tag{2.7}$$

The fully coupled equations of motion are then given by

$$\frac{d\vec{M}}{dt}=\gamma[\vec{M}\times(\vec{H}+\vec{h}_{ls})]-\frac{1}{\tau}\vec{M}\,, \tag{2.8a}$$

$$\vec{\nabla}\cdot\vec{B}=\vec{\nabla}\times\vec{H}=0\,, \tag{2.8b}$$

$$\frac{\partial^2 u_k}{\partial t^2}=\frac{1}{\rho}\sum_i\frac{\partial}{\partial x_i}\frac{\partial}{\partial e_{ki}}(\mathcal{H}+\mathcal{H}_{ls})\,. \tag{2.8c}$$

The effects of exchange have been ignored in the foregoing discussion, since here we are concerned with wavelengths sufficiently long that the dominant

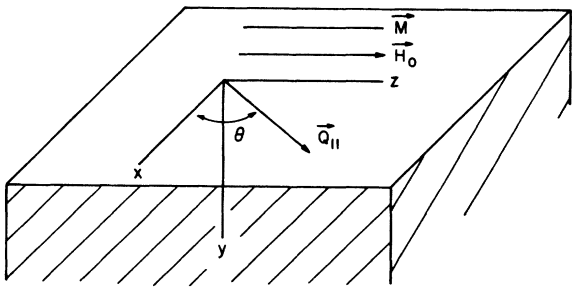

FIG. 1. Propagation geometry considered in the present paper. The magnetization of the ferromagnet is parallel to the surface, as is the externally applied magnetic field.

source of excitation energy of the spin system is the Zeeman energy along the demagnetizing fields generated by the spins.

At the surface of the crystal we require that the usual electromagnetic and mechanical boundary conditions be satisfied. These are the conservation of normal components of $\vec{B}$ and tangential components of $\vec{H}$ across the surface, and the condition that the surface be stress free.

In order to examine the equations of motion Eq. (2.8) and boundary conditions for surface wave solutions, we take the y variation of the lattice displacements and all other dynamical variables to be exponentially damped away from the surface with rate α. Thus, for example,

$$u_x = u_{x0} e^{-\alpha y} e^{i(Q_x x + Q_z z)} e^{-i\Omega t} . \tag{2.9}$$

It is convenient to transform to the lattice displacement coordinates, u_l, u_t, $u_\perp$, defined below. The two quantities u_l and $u_\perp$ are the displacements in the sagittal plane parallel and perpendicular to the surface, while u_t is the displacement perpendicular to the sagittal plane.

$$\begin{aligned} u_x &= u_l \cos\theta - u_t \sin\theta , \\ u_y &= u_\perp , \\ u_z &= u_l \sin\theta + u_t \cos\theta . \end{aligned} \tag{2.10}$$

Upon making these substitutions and expanding Eq. (2.8c), one obtains a system of equations describing the motion of the lattice which also contain the magnetization components:

$$(\Omega^2 + c_t^2\alpha^2 - c_l^2 Q_\parallel^2)u_l - i(c_l^2 - c_t^2)\alpha Q_\parallel u_\perp + (b_2/\rho M_s)(iQ_\parallel \sin 2\theta M_x - \alpha \sin\theta M_y) = 0 , \tag{2.11}$$

$$i(c_l^2 - c_t^2)\alpha Q_\parallel u_l - (\Omega^2 + c_l^2\alpha^2 - c_t^2 Q_\parallel^2)u_\perp - i(b_2/\rho M_s)Q_\parallel \sin\theta M_y = 0 , \tag{2.12}$$

$$(\Omega^2 + c_t^2\alpha^2 - c_t^2 Q_\parallel^2)u_t + (b_2/\rho M_s)(iQ_\parallel \cos 2\theta M_x - \alpha \cos\theta M_y) = 0 . \tag{2.13}$$

From Eq. (2.12) it is evident that, in the presence of magnetoelastic coupling, $u_t \neq 0$ in contrast to the case of pure Rayleigh propagation, where the displacement is confined to the sagittal plane.[4]

The Maxwell equations in Eq. (2.8b) may be combined to form the single equation

$$i(Q_\parallel^2 - \alpha^2)h_z + 4\pi Q_\parallel (iQ_\parallel \sin\theta \cos\theta M_x - \alpha \sin\theta M_y) = 0 . \tag{2.14}$$

Here we have chosen to designate the z component of the demagnetizing field h_z as the fourth dynamical variable.

Finally, the Bloch equation, Eq. (2.8a), provides relations between the components of the magnetization and of the displacement:

$$M_x = \left(\frac{\Omega_M}{\Omega_H^2 - \tilde{\Omega}^2}\right)\left[\Omega_H \cot\theta - \tilde{\Omega}\left(\frac{\alpha}{Q_\parallel}\right)\csc\theta\right]h_z + i\left(\frac{\gamma b_2}{\Omega_H^2 - \tilde{\Omega}^2}\right)[\tilde{\Omega}\alpha \sin\theta - \Omega_H Q_\parallel \sin 2\theta]u_l + i\left(\frac{\gamma b_2}{\Omega_H^2 - \tilde{\Omega}^2}\right)(\tilde{\Omega}\alpha \cos\theta - \Omega_H Q_\parallel \cos 2\theta)u_t + \left(\frac{\gamma b_2 \tilde{\Omega}}{\Omega_H^2 - \tilde{\Omega}^2}\right)Q_\parallel \sin\theta u_\perp , \tag{2.15}$$

$$M_y = i\left(\frac{\Omega_M}{\Omega_H^2 - \tilde{\Omega}^2}\right)\left[\Omega_H\left(\frac{\alpha}{Q_\parallel}\right)\csc\theta - \tilde{\Omega}\cot\theta\right]h_z + \left(\frac{\gamma b_2}{\Omega_H^2 - \tilde{\Omega}^2}\right)(\Omega_H \alpha \sin\theta - \tilde{\Omega} Q_\parallel \sin 2\theta)u_l + \left(\frac{\gamma b_2}{\Omega_H^2 - \tilde{\Omega}^2}\right)(\Omega_H \alpha \cos\theta - \tilde{\Omega} Q_\parallel \cos 2\theta)u_t - i\left(\frac{\gamma b_2 \Omega_H}{\Omega_H^2 - \tilde{\Omega}^2}\right)Q_\parallel \sin\theta u_\perp . \tag{2.16}$$

In these equations $\tilde{\Omega} = \Omega + i/\tau$.

We may eliminate M_x and M_y form Eqs. (2.11)–(2.13) and from Eq. (2.14) to obtain four equations in the variables u_l, u_t, $u_\perp$, and h_z. These equations have a nonzero solution only if the determinant of the coefficients vanishes. This condition provides a polynomial of the eight order in the decay length α.

The explicit expansion of the determinant is very awkward and cumbersome. As a consequence, we have developed a computer routine which performs the expansion on the computer, isolating and keeping track of the prefactors of the various powers of α in the process, to provide the coefficients of the polynomial in the end. The roots of the polynomial in α may then be found numerically. Of these eight roots only four are physically acceptable, with real parts greater than zero. From these four values for the decay constant, α_1, α_2, α_3, α_4, we construct a solution which represents a superposition of waves having as decay paramaters α_1, α_2, α_3, α_4, respectively. For example,

$$u_l = \sum_k u_{l0}^{(k)} e^{-\alpha_k y} e^{i(Q_x x + Q_z z)} e^{-i\Omega t} . \tag{2.17}$$

Similar superpositions are constructed for the remaining dynamical variables and it is these solutions which are submitted to the boundary conditions. Note that the amplitudes $u_l^{(k)}$, $u_t^{(k)}$, $u_\perp^{(k)}$, and $h_z^{(k)}$ are interrelated through the bulk equations Eq. (2.11)–(2.14). Thus, if we choose a value of Ω and $\vec{Q}$, at this point four arbitrary amplitudes re-

main, namely $u_l^{(1)}-u_l^{(4)}$. Further constraints on the solution are found by submitting the solution to the boundary conditions.

If t_{ij} is the i-jth element of the stress tensor, then in the present case the stress-free boundary conditions read

$$t_{xy}=\left(\frac{\partial \mathcal{H}}{\partial e_{xy}}\right)_{y=0}=c_{44}e_{xy}\big|_{y=0}=0\ , \tag{2.18a}$$

$$t_{yy}=\left(\frac{\partial \mathcal{H}}{\partial e_{yy}}\right)_{y=0}=c_{11}e_{yy}+c_{12}(e_{xx}+e_{zz})\big|_{y=0}=0\ , \tag{2.18b}$$

$$t_{zy}=\left(\frac{\partial \mathcal{H}}{\partial e_{yz}}\right)_{y=0}=c_{44}e_{yz}+\frac{b_2}{M_s}M_y\ \Big|_{y=0}=0\ . \tag{2.18c}$$

The presence of the term proportional to b_2 in Eq. (2.18c) will play a critical role, as we shall see. The boundary conditions that require conservation of tangential $\vec{h}$ and normal $\vec{B}$ may be combined into the single statement

$$\sum_k (|Q_{\parallel}|+\alpha_k)h_z^{(k)}-i4\pi Q_{\parallel}\sin\theta\sum_k M_y^{(k)}=0\ . \tag{2.19}$$

The factor $|Q_{\parallel}|$ in Eq. (2.19) has its origin in the fact that outside the substrate ($y<0$), the magnetic field decays in free space like $e^{+|Q_{\parallel}|y}$. This is the source of the nonreciprocity in the dispersion relations we will find subsequently. The four equations in Eqs. (2.18) and (2.19) may be written as four homogeneous equations in the amplitudes $u_l^{(k)}$ by eliminating the other variables $h_z^{(k)}$, $M_y^{(k)}$, ..., through use of the bulk equations quoted earlier. The expressions are cumbersome, and will not be quoted explicitly here.

The entire procedure outlined above has been carried out automatically, by machine. In practice, one chooses the frequency Ω and guesses a value $Q_{\parallel}$. We choose Ω real, and then $Q_{\parallel}$ will be complex, with the attenuation length the inverse of its imaginary part. The computer routine then provides the value of the determinant, $D(\Omega,Q_{\parallel})$, of the coefficients of the boundary condition equations. Our objective then is, for fixed real Ω, to seek the complex values of $Q_{\parallel}$ at which $D(\Omega,Q_{\parallel})=0$. This task, complicated by the fact that $D(\Omega,Q_{\parallel})$ is a complex function of a complex variable, can be programmed with sufficient efficiency and the zeros of $D(\Omega,Q_{\parallel})$ can be found to extremely high accuracy. Using this procedure we are able to calculate the dispersion relation, attenuation length, penetration depths, demagnetizing fields and polarizations of the lattice motion at various angles of propagation. In Sec. III, we present our results.

III. RESULTS OF THE CALCULATIONS

In this section, we present the results of our investigation of the nature of the magnetoelastic surface waves. Before the general results are displayed, it is useful to discuss two special propagation directions, $\theta=\frac{1}{2}\pi$ (propagation parallel to the magnetic field and the magnetization), and $\theta=0$, π (propagation perpendicular to the magnetic field and magnetization). We consider each case separately.

A. Case $\theta = 0$ or π

When $\theta=0$ or π, M_x and M_y drop out of Eqs. (2.11) and (2.12), so these equations involve the two lattice displacements in the sagittal plane only. Furthermore, these two displacement components contribute only to the elements e_{xx}, e_{yy}, and e_{xy} of the strain tensor. As a consequence, the boundary conditions Eqs. (2.18a) and (2.18b) are the only two that involve u_l and $u_\perp$. This set of equations just describe a Rayleigh wave uncoupled to the spins. Thus, for propagation perpendicular to the magnetization, the Rayleigh wave is uncoupled to the spin system. This may be appreciated from Eq. (2.5), where one sees no terms linear in both the transverse magnetization and the strain field set up by the Rayleigh wave.

But as Parekh[1] has pointed out, for propagation perpendicular to the magnetization, a shear polarized magnetoelastic surface wave may propagate. This wave owes its existence to the presence of magnetoelastic coupling, and is a magnetic analog of the Bleustein-Gulyaev wave which may propagate on the surface of a piezoelectric crystal.[5] Here the situation is considerably more interesting than in the piezoelectric case, in that the spin system may exhibit a resonant response to the strain field which drives it. For completeness, we briefly sketch the dispersion relation of this wave.

In the shear polarized surface wave with $\theta=0$ or π, u_l and $u_\perp$ vanish, as does h_z. The amplitudes u_t, M_x, and M_y are nonzero along with h_x and h_y. Since $\nabla\times\vec{h}=0$, as θ approaches 0 or π, we have $h_z=h_x\tan\theta$. If this relation is used in Eqs. (2.15) and (2.16), then with $\sigma=+1$ for $\theta=0$ and $\sigma=-1$ for $\theta=\pi$ we have

$$M_x=\left(\frac{\Omega_M}{\Omega_H^2-\tilde{\Omega}^2}\right)\left[\Omega_H-\tilde{\Omega}\sigma\left(\frac{\alpha}{Q_{\parallel}}\right)\right]h_x + i\left(\frac{\gamma b_2}{\Omega_H^2-\tilde{\Omega}^2}\right)[\tilde{\Omega}\sigma\alpha-\Omega_H Q_{\parallel}]u_t \tag{3.1}$$

and

$$M_y=i\left(\frac{\Omega_H}{\Omega_H^2-\tilde{\Omega}^2}\right)\left[\sigma\Omega_H\left(\frac{\alpha}{Q_{\parallel}}\right)-\tilde{\Omega}\right]h_x + \left(\frac{\gamma b_2}{\Omega_H^2-\tilde{\Omega}^2}\right)[\sigma\Omega_H\alpha-\tilde{\Omega}Q_{\parallel}]u_t\ . \tag{3.2}$$

With these relations, Eq. (2.13) may be written in terms of the two variables u_t and h_x, while the

$\vec{\nabla}\times\vec{h}=0$ and $\vec{\nabla}\cdot\vec{b}=0$ equations are also readily reduced to a single relation between h_x and u_t. The values of α allowed are readily found by equating the 2×2 determinant formed from these equations to zero. This leads to the simple relation

$$(\alpha^2-Q_{\parallel}^2)[\alpha^2-Q_{\parallel}^2+(\Omega^2/c_t^2)\eta_B(\tilde{\Omega})]=0\ , \tag{3.3}$$

where

$$\eta_B(\tilde{\Omega})=[1-\Delta\Omega_H^2/(\Omega_H\Omega_B-\tilde{\Omega}^2]^{-1}\ . \tag{3.4}$$

In Eq. (3.4), the parameter Δ is a dimensionless measure of the strength of the magnetoelastic coupling. It will play a key role throughout the paper. It is given by

$$\Delta=\gamma b_2^2/\rho c_t^2 M_s\Omega_H\ . \tag{3.5}$$

Also, in Eq. (3.4), $\Omega_B=\Omega_H+4\pi\Omega_M$.

The quantity $\eta_B(\tilde{\Omega})$ has a straightforward physical interpretation. It is the acoustical analog of the complex index of refraction of a dispersive medium. In this case, it is the effective index of refraction for propagation of *bulk* transverse magnetoelastic waves, with displacement in the plane perpendicular to the magnetization. This dispersion relation is[3]

$$c_t^2Q^2/\Omega^2=\eta_B(\tilde{\Omega})\ . \tag{3.6}$$

The expression in Eq. (3.3) admits two values of α. For the first ($\alpha=|Q_{\parallel}|$), one has a solution of the bulk equations with $u_t\equiv 0$, but M_x, M_y, and $\vec{h}$ nonzero. For the second, all amplitudes are nonvanishing. These two solutions are mixed by the boundary condition in Eq. (2.18c). After some algebra, one may show that the boundary condition is satisfied only if the dispersion relation

$$c_t^2Q_{\parallel}^2/\Omega^2=\eta_B(\tilde{\Omega})/[1-\gamma^2(\tilde{\Omega})] \tag{3.7}$$

is satisfied, where

$$\gamma(\tilde{\Omega})=\frac{\Delta\Omega_H}{(\Omega_s+\sigma\tilde{\Omega})}\frac{(\tilde{\Omega}+\sigma\Omega_>)(\tilde{\Omega}-\sigma\Omega_<)}{[\tilde{\Omega}^2-\Omega_H(\Omega_B-\Delta\Omega_H)]}\ . \tag{3.8}$$

In the limit where the spin damping is ignored ($\tau\to\infty$), then the surface mode exists only for frequencies where $0<\gamma(\Omega)<1$.

In Eq. (3.8), $\Omega_s=\frac{1}{2}(\Omega_H+\Omega_B)$ is the frequency of the Damon-Eshbach surface spin wave, for propagation perpendicular to the magnetization. We remind the reader that (in our geometry), the Damon-Eshbach wave propagates only from right to left, but not from left to right. It is a simple example of a wave with a nonreciprocal dispersion relation, a feature we will see reflected in the more complex magnetoelastic waves that form the topic of the present paper. Also, the frequencies $\Omega_>$ and $\Omega_<$ are

$$\Omega_>=\tfrac{1}{2}\{[\Omega_H(\Omega_H+8\pi\Omega_M)]^{1/2}+\Omega_H\}\ , \tag{3.9a}$$

$$\Omega_<=\tfrac{1}{2}\{[\Omega_H(\Omega_H+8\pi\Omega_M)]^{1/2}-\Omega_H\}\ . \tag{3.9b}$$

We see that like the Damon-Eshbach wave itself, the shear polarized magnetoelastic wave has a nonreciprocal dispersion relation. This follows from the explicit appearance of σ in Eq. (3.8).

In the absence of spin damping, and in the limit of zero magnetic field, the dispersion relation in Eq. (3.7) reduces to the simple form

$$c_t^2Q_{\parallel}^2/\Omega^2=(\Omega+\sigma\Omega_s)^2/[(\Omega+\sigma\Omega_s)^2-\delta^2]\ , \tag{3.10}$$

where $\delta=\Delta\Omega_H$, a quantity independent of H. This dispersion relation is illustrated in Fig. 2, for both directions of propagation. The nonreciprocal character of the dispersion relation is most striking. Figure 3 illustrates the character of the dispersion relation for both senses of propagation, when the Zeeman field is nonzero. For each direction of propagation, there are two branches to the dispersion relation. The cross hatched areas of Fig. 3 are regimes where bulk magnetoelastic waves may propagate, with wave-vector component

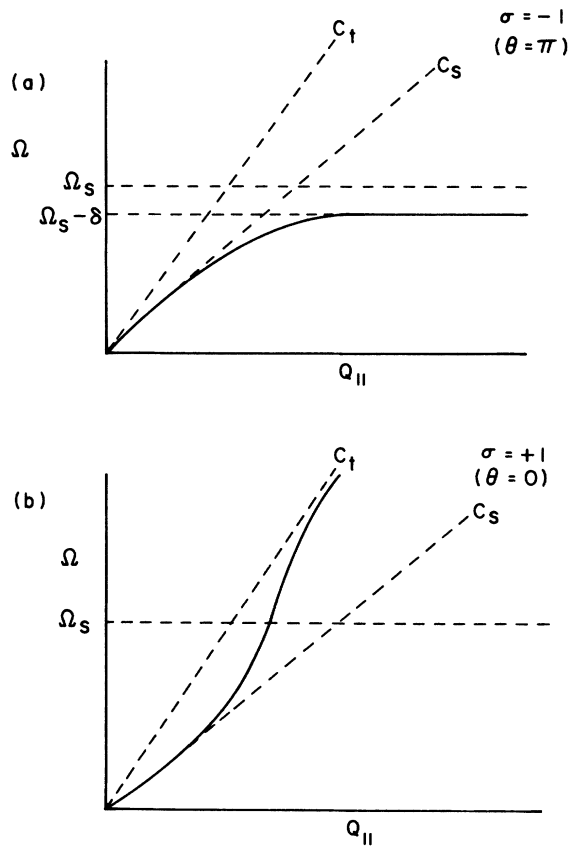

FIG. 2. Dispersion relation for the shear polarized magnetoelastic surface wave for propagation perpendicular to the magnetization. Here the external magnetic field is zero. (a) The propagation direction is from right to left; (b) from left to right.

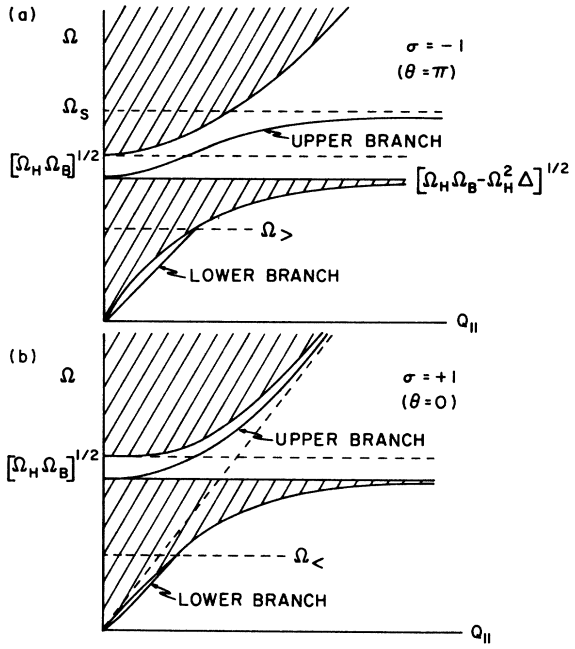

FIG. 3. Dispersion relation for the shear polarized magnetoelastic surface wave for propagation perpendicular to the magnetization, when the external magnetic field is nonzero. (a) The propagation direction is from right to left; (b) from left to right.

$Q_{\parallel}$ parallel to the surface and arbitrary component normal to the surface.

We call attention to the fact that the scales in Figs. 2 and 3 are exaggerated to give a qualitative feel for the nature of the dispersion relations. We shall see for material parameters used below that $\gamma(\Omega)$ is very close to unity, so the dispersion curves lie much too close to the bulk magnetoelastic wave dispersion curve to illustrate on graphs with this scale, except for frequencies very close to Ω_s.

B. Case $\theta = \pm\frac{1}{2}\pi$

We next consider the case $\theta = +\frac{1}{2}\pi$ or $\theta = -\frac{1}{2}\pi$, i.e., propagation either parallel or antiparallel to both the magnetization and the external magnetic field. This case has been considered previously with neglect of spin damping by Parekh and Bertoni, and previously by us with spin damping included.[1] We present a brief summary of the results here for completeness.

For propagation in the direction $\theta = \pm\frac{1}{2}\pi$, the dispersion relation is an even function of $Q_{\parallel}$. We shall see that this follows from very general considerations. For $\theta = \pm\frac{1}{2}\pi$, all the amplitudes are nonzero and coupled. We find a Rayleigh wavelike mode in this propagation geometry, but no analog of the shear-polarized magnetoelastic surface wave of Sec. III A. Here we have a Rayleigh wave which couples to the spins. The spins react back on the lattice with the consequence that $u_t \neq 0$ in addition to u_l and $u_\perp$. Thus, the lattice displacement is no longer confined to the sagittal plane.

In Fig. 4, we present results for the attenuation constant and the real part of $Q_{\parallel}$ for the wave, for propagation on YIG in a magnetic field of 50 G. We comment on the parameters chosen, since these will be used throughout the remainder of the paper. A field of 50 G places the frequency $\Omega_H/2\pi$ at about 100 MHz, a frequency convenient for surface propagation studies. In YIG, this gives $\Omega_B/\Omega_H = 7$, and $\Delta = 9.1 \times 10^{-3}$. The numbers were employed in our previous paper[1] and the earlier work by Parekh and Bertoni.[1] In addition we take the dimensionless parameter $\Gamma = (\Omega_H \tau)^{-1}$ to assume the value 0.01. The results displayed in Fig. 4 are calculated for this value of Γ, and the effect of varying the damping rate has been explored in our previous paper. There we found that the height of the atten-

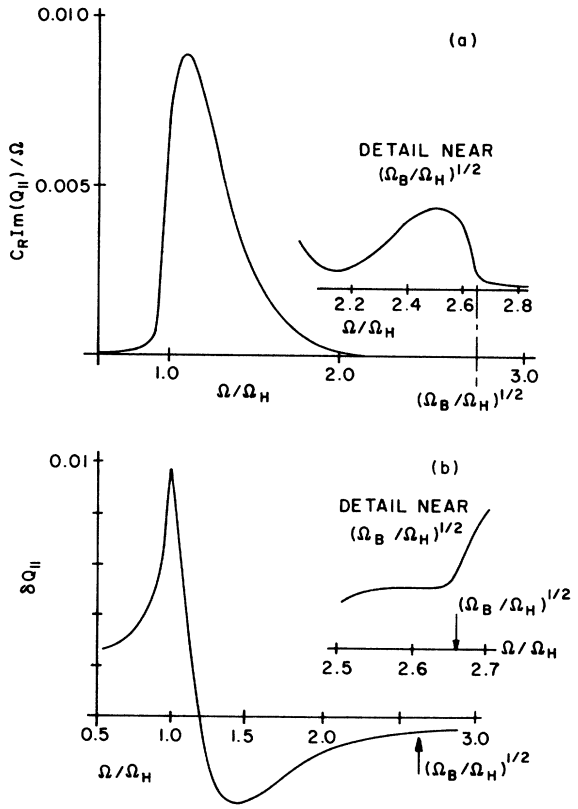

FIG. 4. Frequency variation of the (a) attenuation constant and (b) the real part of the wave vector for a Rayleigh wave which propagates parallel to the magnetization. In (b) the quantity plotted on the vertical axis is $\delta Q_{\parallel} = (C_R Q_{\parallel}^{(R)}/\Omega) - 1$, where $Q_{\parallel}^{(R)}$ is the real part of $Q_{\parallel}$. The parameter $\Gamma = (\Omega_H \tau)^{-1}$, while Δ, Ω_H, and Ω_B are chosen for YIG in a 50-G magnetic field.

uation was sensitive to Γ, but its width is insensitive. This is because, as discussed before, the broad attenuation peak has its origin not primarily in dissipation in the spin system, but in leakage of energy to bulk magnetoelastic waves. The attenuation constant of the Rayleigh wave is quite large at the peak. It assumes a value roughly 30 cm^{-1} at its peak value. Note that in the attenuation constant, the large peak lies a bit above Ω_H, while there is a considerably smaller peak near $(\Omega_H\Omega_B)^{1/2}$, as shown in the inset. A physical argument which explains this behavior may be found in our earlier work.[1]

We next turn to presentation of the results for the case of general propagation direction. Before we do this, we pause to comment on the origin of the nonreciprocity in the surface-wave dispersion relation. We have seen two examples of this nonreciprocal behavior. The first is provided by the Damon-Eshbach spin wave (the surface spin wave present in the absence of magnetoelastic coupling) and the second is the shear polarized magnetoelastic surface wave. A third example is the propagation of surface polaritons in a doped semiconductor placed in a magnetic field parallel to the surface, for the case where the mode propagates perpendicular to the magnetic field.[6]

In all these cases, the *surface*-wave dispersion relation is nonreciprocal, while the dispersion relations of the corresponding *bulk* waves are described by a function even in the wave vector. There is a simple symmetry argument that leads one to appreciate the reason why this is so.

Consider a cubic material, infinite in extent, with magnetic field parallel to the z direction. Let $\Omega_v(k_xk_z)$ be the dispersion relation for a bulk excitation (a polariton, a magnetoelastic wave, ...). We show that $\Omega_v(k_xk_z)$ is an even function of both k_x and k_z. First reflect the whole system through the x-y plane. This changes k_z to $-k_z$, but does *not* change the direction of the magnetic field, since it transforms like a pseudovector under reflection. Since the operation reverses the sign of k_z and leaves both the crystal and magnetic field invariant, we have $\Omega_v(k_x,k_z)=\Omega_v(k_x,-k_z)$. A reflection in the y-z plane changes the sign of k_x. But since the magnetic field is a pseudovector, reflection in a plane *parallel* to the magnetic field changes its sign. The operation is thus not a symmetry operation of the system. Now if we next reflect in the x-z plane, k_x and k_z are unaffected, while the magnetic field is restored to its original direction. Thus, the combination of the two operations is a symmetry operation, and leads us to conclude that $\Omega_v(k_x,k_z)=\Omega_v(-k_x,k_z)$, i.e., the dispersion relation is reciprocal for the bulk mode.

Now consider a surface mode with dispersion relation $\Omega_s(k_x,k_z)$. Again a magnetic field is parallel to the z axis, as in Fig. 1. By precisely the argument given above, we may prove $\Omega_s(k_x,k_z)=\Omega_s(k_x,-k_z)$. However, we cannot prove $\Omega_s(k_x,k_z)$ is even in k_x, because the reflection through the x-z plane is no longer a symmetry operation. It takes a crystal initially in the half-space $y>0$ and flips it into the half-space $y<0$. Thus, $\Omega_s(k_xk_z)\neq\Omega_s(-k_xk_z)$ because of the surface.

This argument applies to all three examples cited above, and leads to an understanding why the bulk wave dispersion relations are even functions of wave vector in the magnetic field, but the surface waves are described by a nonreciprocal form.

With this in mind, we turn to the case of general angle of propagation.

C. General angle of propagation relative to the field

In this section, we describe the results we have obtained for propagation at general angle to the magnetic field. In all the calculations reported below, the parameters used to generate the curves in Fig. 4 have been employed. We shall comment on the sensitivity of the features to the presence of spin damping, although the results presented apply only to the case $(\Omega_H\tau)^{-1}=\Gamma=10^{-2}$.

For each angle of propagation, we find a solution of the equations which may be described as a Rayleigh wave modified in character by the magnetoelastic coupling. That is to say, in contrast to the shear polarized wave examined in Sec. III B, this wave reduces to an ordinary Rayleigh wave in the limit of vanishing magnetoelastic coupling. As we saw in our discussion of propagation parallel to the magnetization and external field, the presence of magnetoelastic coupling introduces a contribution to the lattice displacement perpendicular to the sagittal plane. For $\theta=\frac{1}{2}\pi$, calculations of the magnitude of this displacement are displayed in our earlier paper.

In Fig. 5, we show the variation of the attenuation constant of the wave with frequency, for a large number of angles between $\theta=0$ and $\theta=\pi$. In Fig. 5(a), we show angles in the range $0<\theta<\frac{1}{2}\pi$, and in Fig. 5(b), $\frac{1}{2}\pi<\theta<\pi$. The ordinate is the dimensionless quantity $c_R\,\mathrm{Im}\,(Q_{\parallel})/\Omega_H$, where c_R is the Rayleigh-wave velocity, in the absence of magnetoelastic coupling. Recall from the symmetry argument given above that the curves for $-\pi<\theta<0$ are the same as those for $0<\theta<\pi$.

There are several striking features of these results. First, the nonreciprocal nature of the attenuation constant is evident. For example, one sees sharp spikes (with origin to be discussed below) just above the $(\Omega_H\Omega_B)^{1/2}$ in Fig. 5(b), while these features are absent in Fig. 5(a). Also note

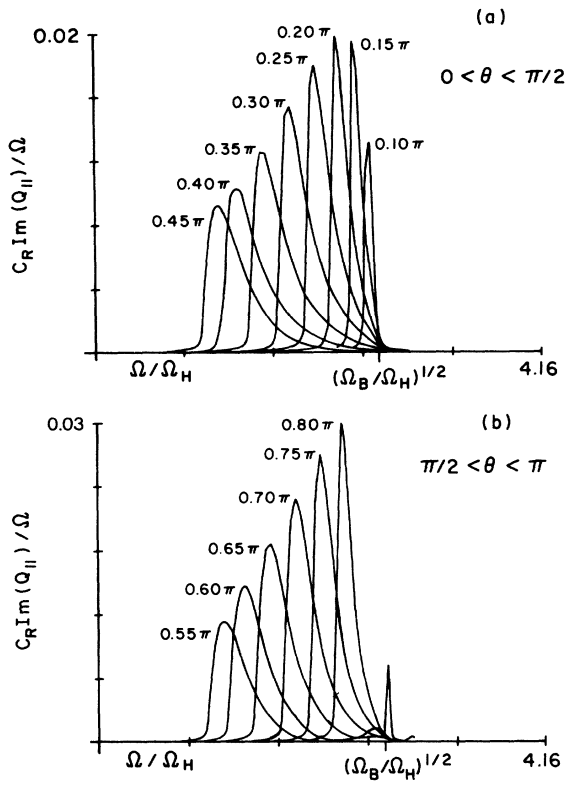

FIG. 5. Attenuation constant for the Rayleigh-wave-like mode, calculated for the parameters used to generate Fig. 4. We show results for propagation angles θ (see Fig. 1) for (a) $0<\theta<\pi$. The nonreciprocal character of the attenuation constant is evident.

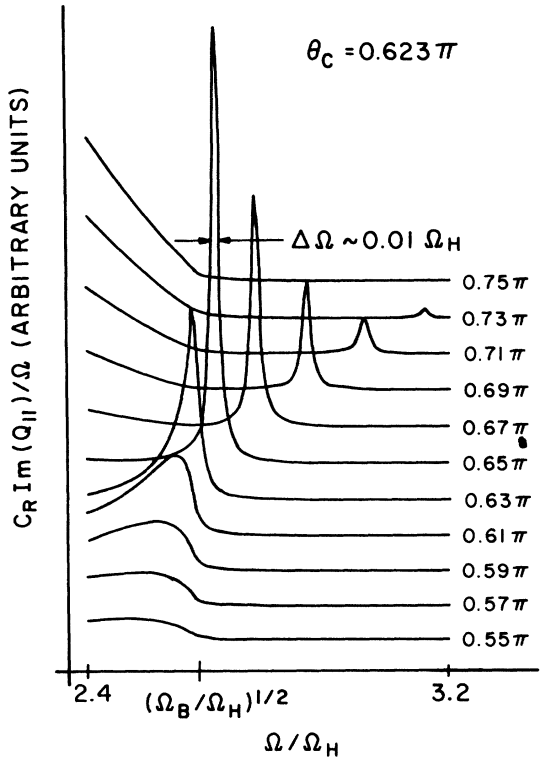

FIG. 6. Enlarged view of the coupling between the Rayleigh wave and the Damon-Eshbach surface spin wave. This is a blow up of the region just above the frequency $(\Omega_H\Omega_B)^{1/2}$ of Fig. 5(b), with many more values of θ included. The values of θ are near the critical angle θ_c where the Damon-Eshbach wave breaks off from the bulk manifold.

the magnitude of the attenuation constant. The heights of the main attenuation peaks between the frequencies Ω_H and $(\Omega_H\Omega_B)^{1/2}$ are also very asymmetrical (note the scales on the vertical axes), with the Rayleigh wave much more strongly attenuated at the angle $\theta=\frac{1}{2}\pi+\xi$ when compared with the angle $\theta=\frac{1}{2}\pi-\xi$. We comment now on the origin of the various features in the attenuation constant.

The sharp peaks above the frequency $(\Omega_H\Omega_B)^{1/2}$ evident in Fig. 5(b) arise from the coupling of the Rayleigh wave to the Damon-Eshbach surface spin wave. Since it is hard to follow the curves in this region as they are presented in Fig. 5(b), we present an enlarged view of these peaks in Fig. 6. Before we interpret these results in detail, we remind the reader of the properties of the Damon-Eshbach surface wave.

The Damon-Eshbach wave propagates on the surface of a semiinfinite ferromagnet, when the magnetization lies parallel to the surface. It propagates in the long-wavelength regime (of interest here) where the exchange energy is negligible.[2] Its propagation characteristics are highly nonreciprocal, in that it propagates only when its wave vector lies in the regime $\theta=\pi\pm\varphi_c$, where $\varphi_c=\cos^{-1}(H/B)^{1/2}$. The dispersion relation of the mode is

$$\Omega_s(\varphi)=\tfrac{1}{2}(\Omega_H/\cos\varphi+\Omega_B\cos\varphi)\ . \tag{3.11}$$

Thus, at $\varphi=\varphi_c$, $\Omega_s(\varphi_c)=\gamma(HB)^{1/2}$, the top of the bulk spin-wave manifold, and as φ is decreased from φ_c, $\Omega_s(\varphi)$ increases to the value $\frac{1}{2}(\Omega_H+\Omega_B)$ at $\varphi=0$. We call the reader's attention to Fig. 3 of the original paper by Damon and Eshbach, which is a very beautiful illustration of how the Damon-Eshbach wave splits off the manifold of bulk spin waves as φ is lowered through φ_c toward zero (note their definition of φ differs from ours by 90°).

The attenuation peaks in Fig. 6 are caused by coupling of the Damon-Eshbach wave to the Rayleigh wave. One sees the Damon-Eshbach wave split off from the bulk manifold just after the critical angle $\theta_c=0.623\pi$, and move up in frequency to produce a sharp attenuation peak. The width of the peak in frequency is proportional to $1/\tau$, so as spin damping is decreased each peak sharpens up and

increase in intensity in a manner typical of Lorentzian absorption lines. For the value of τ we have used (again $\Omega_H\tau = 100$), the width of the absorption line at half-maximum at $\theta = 0.65\pi$ is found to be $\Delta\Omega \approx 0.01\Omega_H$. One striking feature of these results is that as θ increases beyond θ_c towards π, the strength of the attenuation peak from the Damon-Eshbach wave falls off very rapidly with θ. Nonetheless near θ_c, the attenuation from the Damon-Eshbach wave is strong, and the propagation of the Rayleigh wave can readily be manipulated by varying either the magnetic field strength or direction for frequencies near this peak.

We next turn to a discussion of the broad attenuation peaks that lie between the frequency Ω_H and $(\Omega_H\Omega_B)^{1/2}$. We first remark that the peak from coupling to the Damon-Eshbach wave arises because the Rayleigh wave drives the spin system in a resonant manner for frequencies near $\Omega_s(\theta)$, and the presence of the damping leads to local dissipation of energy (heating) by the spin system. The frequency region between Ω_H and $(\Omega_H\Omega_B)^{1/2}$ is a regime where bulk spin waves may propagate. Here the Rayleigh wave is attenuated because the energy in the wave is *radiated* into the bulk of the crystal, with the energy carried off by the bulk spin waves. (This language is somewhat loose; the energy is radiated into the interior, and carried off by bulk magnetoelastic waves; the process is most effective in the frequency domain where these bulk waves have a strong admixture of spin-wave character.) We discussed this process in our first publication, where we showed that shape and intensity of this feature (for $\theta = \frac{1}{2}\pi$) are relatively insensitive to the magnitude of τ.

A simple argument leads one to understand why this main attenuation peak is broadest at $\theta = \frac{1}{2}\pi$, and narrows in width as θ approaches either 0 or π. The Rayleigh wave radiates its energy to bulk spin waves, to speak crudely. The only bulk spin waves a Rayleigh wave of wave vector $\vec{Q}_\parallel$ couples to are those with (three dimensional) wave vector $\vec{Q} = \vec{Q}_\parallel + \hat{y}Q_y$, where $\vec{Q}_\parallel$ is fixed, but Q_y is arbitrary. This follows from the fact that translational invariance parallel to the surface remains, but the translational symmetry normal to the surface is broken. The spin-wave dispersion relation for a bulk spin wave of wave vector $\vec{Q} = \vec{Q}_\parallel + \hat{y}Q_y$ is given by the well-known expression[7] (adapted to our notation)

$$\Omega_v(\vec{Q}) = \left\{\Omega_H\left[\Omega_H + 4\pi\Omega_M\left(1 - \frac{Q_\parallel^2\sin^2\theta}{Q_\parallel^2 + Q_y^2}\right)\right]\right\}^{1/2}. \tag{3.12}$$

As Q_y varies from zero to infinity, $\Omega_v(\vec{Q})$ ranges from a minimum of

$$\Omega_v^{(m)} = [\Omega_{\perp}(\Omega_H + 4\pi\Omega_M\cos^2\theta)]^{1/2}$$

to a maximum of $\Omega_v^{(M)} = (\Omega_H\Omega_B)^{1/2}$. Thus, as θ approaches either 0 or π, the frequency regime within which the radiation process can occur shrinks to a narrow band just below $(\Omega_H\Omega_B)^{1/2}$, so we expect a peak there. For $\theta = \frac{1}{2}\pi$, the radiation damping can occur throughout the range $\Omega_H < \Omega < (\Omega_H\Omega_B)^{1/2}$, and in our previous paper we present a physical argument which shows the largest peak should lie near Ω_H, with only weak structure near $(\Omega_H\Omega_B)^{1/2}$. This physical reasoning leads us to understand the principal trends in the computer results.

Our final comment concerns the physical origin of the strong asymmetry about $\theta = \frac{1}{2}\pi$ in the height of the attenuation peak in the "radiation damping" region between Ω_H and $(\Omega_H\Omega_B)^{1/2}$. At any point in space, the transverse magnetization vector $\hat{x}M_x + \hat{y}M_y$ traces out an ellipse. The same is true for the displacement field associated with the Rayleigh wave. The attenuation peak is strongest when both the magnetization and displacement fields transverse their respective ellipses in the same sense. This happens for $\frac{1}{2}\pi < \theta < \pi$. For $0 < \theta < \frac{1}{2}\pi$, the two vectors precess in the opposite sense, with the result that the Rayleigh wave couples less efficiently to the spins.

When the attenuation constant is strongly frequency dependent, general considerations lead one to expect the presence of anomalous dispersion in the wave. We have calculated the frequency variation of the real part of the wave vector of the Rayleigh-like surface magnetoelastic wave, and we turn to these results next. In Fig. 7, we show the frequency variation of the real part of the wave vector of the Rayleigh-wave-like mode. The dispersion introduced by coupling to the bulk spin-wave modes, and that introduced by coupling to the Damon-Eshbach mode is evident. The quantity displayed on the vertical axis is the dimensionless variable $(c_R Q_\parallel^{(R)}/\Omega) - 1$, where $Q_\parallel^{(R)}$ is the real part of the wave vector of the mode. In Fig. 8, we show an expanded series of plots which illustrate the behavior of the real part of the wave vector near the angle and frequency range where coupling to the Damon-Eshbach wave exists.

In our previous paper,[1] for $\theta = \frac{1}{2}\pi$, we presented graphs of the magnitude and frequency variation of $u_\perp$ and h_z at the crystal surface. We have extended these calculations to the case of arbitrary propagation angle. The details are presented elsewhere.[8]

The final topic we discuss is the behavior of the shear polarized surface wave discussed in Sec. III A. For θ near π, we have explored the behavior of the branch in Fig. 3(a) which lies between $(\Omega_H\Omega_B)^{1/2}$ and Ω_s. We remark that this is a most

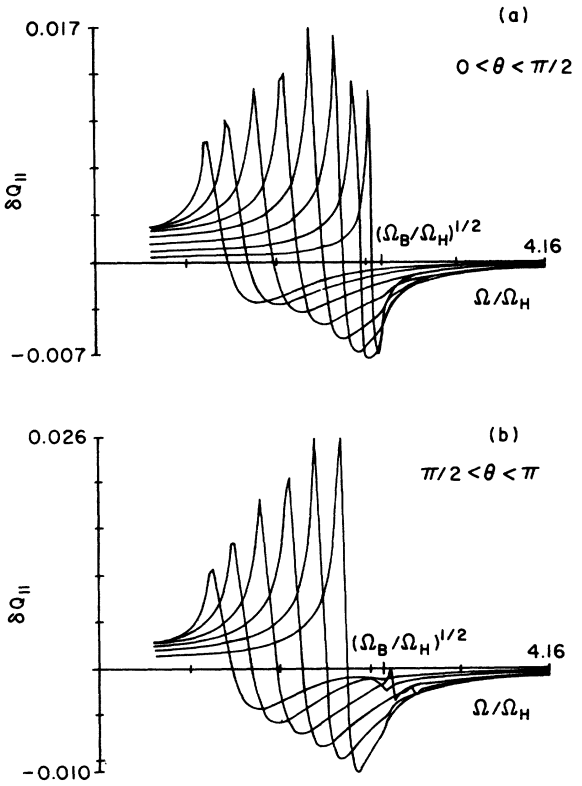

FIG. 7. Frequency variation of the real part of the wave vector of the Rayleigh-wave-like mode, calculated for the parameters used to generate Fig. 4. We show results for propagation angles θ (see Fig. 1) for (a) $0 < \theta < \frac{1}{2}\pi$ and (b) $\frac{1}{2}\pi < \theta < \pi$. The nonreciprocal character of the dispersion is evident. The quantity plotted on the vertical axis is $\delta Q_{\parallel} = (C_R Q_{\parallel}^{(R)}/\Omega) - 1$, where $Q_{\parallel}^{(R)}$ is the real part of the wave vector.

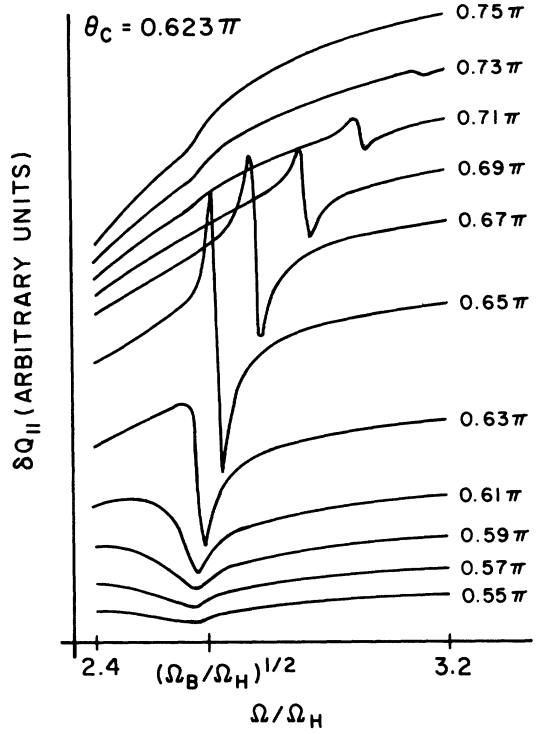

FIG. 8. Expanded view of the frequency variation of the real part of the wave vector of the Rayleigh wave, in the frequency regime just above $(\Omega_H \Omega_B)^{1/2}$. This shows the effect of coupling to the Damon-Eshbach wave on the real part of the wave vector.

difficult task since, as we stated earlier, the surface-wave dispersion relation lies extremely close to that of a shear polarized bulk magnetoelastic wave which propagates parallel to the surface. Thus, the task of obtaining the surface-wave dispersion relation by numerical methods requires great accuracy in the computer routine. First, it is important to note the wave is shear polarized only at $\theta \equiv \pi$. As θ deviates from π, the amplitudes $u_\perp$ and u_t become nonzero, although the wave remains very predominantly shear polarized in character.

Basically, we find the dispersion relation is affected in a strong and pronounced manner, when θ deviates only a small amount from π. As we saw earlier, for $\theta = \pi$, the frequency lies very close to that of the bulk magnetoelastic waves which propagate parallel to the surface. We find as θ deviates from π a small amount, the upper-branch surface-wave dispersion curves begin to intersect their corresponding bulk magnetoelastic wave dispersion curves at finite values of $Q_{\parallel} = Q_{\parallel}^{(c)}(\theta)$, where $Q_{\parallel}^{(c)}(\theta)$ is a strong function of θ. In the absence of damping, at $\theta = \pi$, $Q_{\parallel}^{(c)}(\pi)$ is infinite. For $Q_{\parallel} > Q_{\parallel}^{(c)}(\theta)$ and $\theta \neq \pi$, we find a region of frequencies wherein there are no solutions to the equations. The dispersion curves are then found to reemerge at a higher frequency thus introducing a gap in the shear polarized magnetoelastic surface-wave dispersion curve for θ sufficiently removed from π. This behavior is illustrated schematically in Fig. 9. Note that the dispersion curves for angles of propagation θ greater than θ' in Fig. 9, are interrupted and possess a gap. Further, the gap width $W(\theta)$ is a strong function of θ.

To illustrate these points, we begin with a curve for the case $\theta = 0.99\pi$. In Fig. 10(a), we show the frequency variation of the real part of the wave vector at $\theta = 0.99\pi$, and the imaginary part is displayed in Fig. 10(b). Since $0.99\pi > \theta'$ of Fig. 9, the dispersion curve in Fig. 10(a) looks very much like the upper branch in Fig. 3(a), once it is realized that the effect of damping produces the hairpinlike bends such as that near $(\Omega_H \Omega_B)^{1/2}$ in Fig. 10(a).[9] We presume a similar hairpinlike behavior

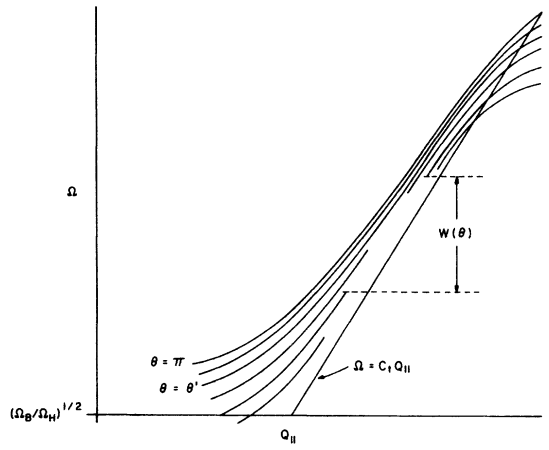

FIG. 9. Schematic representation of the dispersion of the shear polarized wave for angles of propagation near π. For angles $\theta' < \theta < \pi$ the branch is qualitatively similar to the upper branch in Fig. 3 (a). For $\theta' > \theta$, the curves exhibit gaps of width $W(\theta)$. For the parameters of YIG, $\theta' \approx 0.984\pi$.

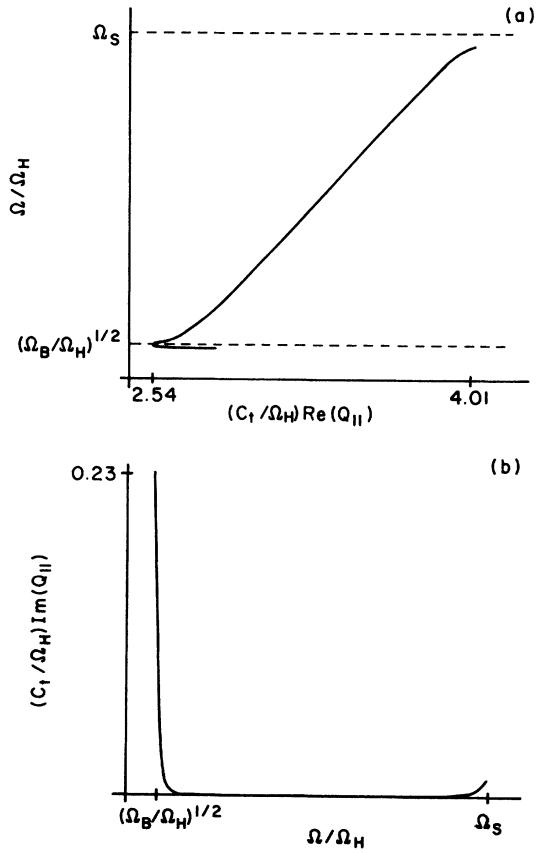

FIG. 10. Dispersion curve for the shear polarized magnetoelastic surface wave, at $\theta = 0.99\pi$. Here, $\theta' < \theta$. The parameters used are those employed to construct Fig. 4. We show (a) the frequency variation of the real part of the wave vector, and (b) the imaginary part.

occurs at the high-frequency extremum of the dispersion curve. This is hard for us to resolve numerically, because the upper hairpin is quite sharp; one is far from the bulk ferromagnetic resonance frequency (in terms of the presumed linewidth), and the hairpin is hard to trace and follow with our routine that searches for wave vectors associated with a fixed frequency.

In Fig. 11, the upper branch is shown for $\theta = 0.95\pi$. Here, $0.95\pi < \theta'$ of Fig. 9 and it is clear that the mode cuts off at finite wave vector. In our numerical calculations, which calculate the complex wave vector of the mode in frequency increments $\Delta\Omega = 10^{-3}\Omega_H$, the termination of the dispersion relation is sufficiently abrupt that with our search routine, we do not find a root at the first frequency increment beyond the cutoff frequency. The reason for the abrupt cutoff is that the surface mode dispersion relation intersects the dispersion curves for the bulk magnetoelastic waves at finite wave vector, when θ differs only a small amount from π. We illustrate this in Fig. 11 by superimposing on the figure the bulk magnetoelastic wave dispersion curve in the form of a dotted line. This curve describes the shear polarized bulk magnetoelastic wave, with lattice displacement parallel to the magnetization. This dispersion curve is a plot of frequency versus the magnitude of the wave vector of the mode, for the case where the bulk wave

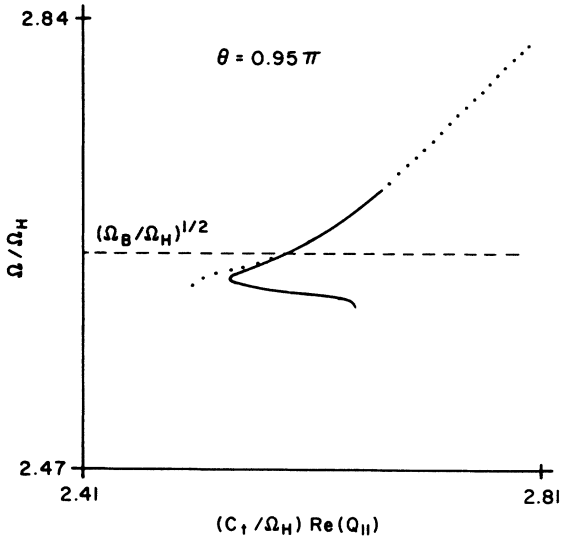

FIG. 11. Upper branch of the shear polarized magnetoelastic dispersion curve for $\theta = 0.95\pi$. Here, $\theta < \theta'$. Note that the upper end of the dispersion curve cuts off suddenly at finite wave vector. Superimposed on the graph is the upper branch of the bulk shear polarized magnetoelastic wave (displacement parallel to $\hat{z}$) with $Q_y = 0$, and wave vector parallel to the surface with $\theta = 0.95\pi$.

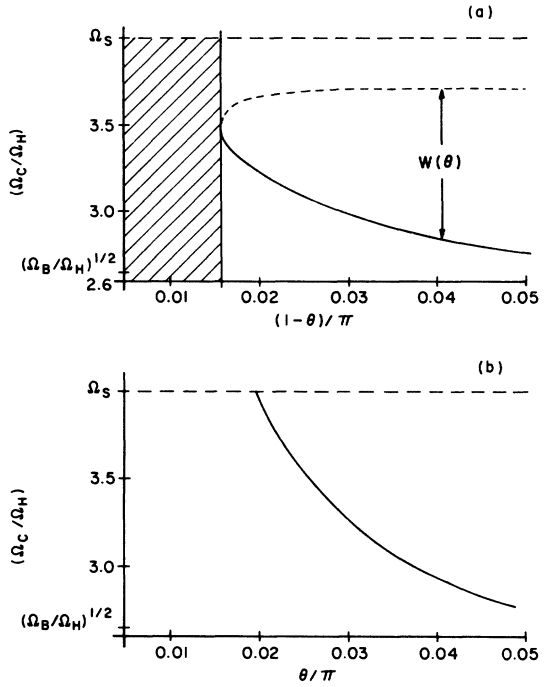

FIG. 12. Angular variation of the cutoff frequency Ω_c, and the frequency of the reemergence of the upper branches of the shear polarized magnetoelastic surface wave. We show (a), for θ near π, the angular variation of the cutoff frequency (solid line) and the angular variation of the frequency at which the mode reappears (dashed line). In the shaded region the dispersion curves are uninterrupted while those dispersion curves to the right of the shaded region exhibit a gap of width $W(\theta)$. The right-hand boundary of the shaded portion corresponds to θ' which is approximately 0.984π for the YIG parameters employed here.

propagates parallel to the surface, with wave vector along the line $\theta = 0.95\pi$ in the x-z plane. (As with the surface wave, the mode is purely shear polarized only when $\theta = \pi$. For $\theta = 0.95\pi$, it is predominantly a shear mode, however.) In our numerical work, we have compared the cutoff wave vector of the surface mode with the wave vector of the bulk wave of the appropriate frequency, and two agree very well.

We find this cutoff behavior a general feature of the transverse magnetoelastic surface wave branch, when θ differs from π. In Fig. 12(a) we show the angular variation of the cutoff frequency and the frequency at which the dispersion curves reemerge.

In Fig. 3, for $\theta = 0$, there is also an upper branch of the shear polarized magnetoelastic surface-wave dispersion relation illustrated. In this case, the curve approaches $\Omega = c_t Q_{\parallel}$ as $Q_{\parallel} \to \infty$. We find for propagation angles near zero, this branch also cuts off at finite wave vector, after intersecting the bulk magnetoelastic wave band. In Fig. 12(b), we plot the angular variation of the cutoff frequency for this branch.

Our conclusion is then that while the shear polarized magnetoelastic waves exist at $\theta = 0$ and π very clearly, they have propagation characteristics very sensitive to small deviations from either $\theta = 0$ and $\theta = \pi$.

IV. CONCLUSIONS

In this paper, we have traced out the behavior of magnetoelastic surfaces on a ferromagnet with magnetization parallel to the surface, for arbitrary angle between the magnetization and the propagation direction. The calculations reveal a rich complex of behavior. In the case of the Rayleigh-like magnetoelastic surface wave, we have seen the striking nonreciprocity in the frequency variation of the attenuation constant. This is evident from the behavior of the "radiation damping" that results from leakage of energy to the bulk magnetoelastic waves, and from the attenuation peak produced by coupling to the Damon-Eshbach mode. We have also found the propagation characteristics of the shear polarized surface waves to be very sensitive to the propagation direction.

These waves should prove a most useful probe of spin dynamics in the near vicinity of the surface of a ferromagnet. We believe this should prove a most interesting area of experimental research. One has here a short-wavelength probe of the nature of spin excitations very near the surface that offers advantages complementary to microwave studies, which require thin film samples for the study of spin pinning near surfaces. It is our hope that the present paper will stimulate further thought in this area by experimentalists.

---

*Work supported by the Air Force Office of Scientific Research, Grant No. AFOSR 76-2887, Office of Aerospace Research, U.S.A.F.

[1]There have been several discussions of surface magnetoelastic waves in the literature, but until the present work, no discussion of the propagation of the waves at arbitrary angles to the field has been presented, for a free surface. We shall see that very rich structure emerges in this case. In earlier papers, Parekh and his collaborators explore a variety of propagation geometries with boundary conditions that presume a perfectly conducting but massless film on the magnetic

substrate. See J. P. Parekh, in *Proceedings of 1972 IEEE Ultrasonics Symposium* (IEEE, Boston, 1972), p. 333; J. P. Parekh and H. L. Bertoni, Appl. Phys. Lett. 20, 362 (1972); and S. Shen, J. P. Parekh, and G. Thomas, in *Proceedings of 1974 IEEE Ultrasonics Symposium* (IEEE, Boston, 1972), p. 483). Unfortunately, use of the metallized boundary condition suppresses the Damon-Eshbach surface spin wave. On the free surface, propagation of transverse magnetoelastic surface waves perpendicular to the magnetization has been discussed by J. P. Parekh [Electron. Lett. 6, 430 (1970)], and the propagation of Rayleigh waves parallel to the field has been examined by J. P. Parekh and H. L. Bertoni [J. Appl. Phys. 45, 434 (1974)] and R. Q. Scott and D. L. Mills [Solid State Commun. 18, 7 (1976).

[2]R. W. Damon and J. R. Eshbach, J. Phys. Chem. Solids 19, 308 (1960).

[3]C. Kittel, Phys. Rev. 110, 836 (1958).

[4]See, L. D. Landau and E. M. Lifshitz, *Theory of Elasticity*, 2nd ed. (Pergamon, Oxford, 1970), p. 101.

[5]J. L. Bleustein, Appl. Phys. Lett. 13, 412 (1968); Y. V. Gulyaev, Zh. Eksp. Teor. Fiz. 9, 1 (1969) [Sov. Phys.-JETP Lett. 9, 37 (1969)].

[6]See J. J. Brion, R. F. Wallis, A. Hartstein, and E. Burstein, Phys. Rev. Lett. 28, 1455 (1972). The dispersion relation of these waves has been studied experimentally by A. Hartstein and E. Burstein [Solid State Commun. 14, 1223 (1974)].

[7]See the result in Eqs. (108) and (110) of C. Kittel, *Quantum Theory of Solids* (Wiley, New York, 1964), p. 67. It is necessary to ignore the effect of exchange and anisotropy in this formula.

[8]R. Q. Scott, thesis (University of California at Irvine, 1976) (unpublished).

[9]See Fig. (14) on p. 39 of A. S. Barker and R. Loudon, Rev. Mod. Phys. 44, 18 (1972).